

Article

Construction of a Novel Chimeric Dextranucrase Fused to the Carbohydrate-Binding Module CBM2a

Reinaldo Fraga Vidal ^{1,*} , Roberto Carlos Arísticas Ribalta ¹, Lisandra Teresa Martínez Valdés ¹, Meinardo Lafargue Gámez ¹, Amanda Montes Alvarez ¹, Arianne Rubio Sánchez ¹, Eric Dubreucq ² , and Benoît Moreau ³

- ¹ Department of Microbiology and Genetics, Cuban Research Institute on Sugarcane By-Products (ICIDCA), P.O. Box 4026, Havana 11000, Cuba; roberto.aristicas@icidca.azcuba.cu (R.C.A.R.); lisandra.martinez@icidca.azcuba.cu (L.T.M.V.); meinardo.lafargue@icidca.azcuba.cu (M.L.G.); amanda.montes@icidca.azcuba.cu (A.M.A.); arianne.rubio@icidca.azcuba.cu (A.R.S.)
² IATE, Institut Agro, INRAE, Univ. Montpellier, 34060 Montpellier, France; Eric.Dubreucq@supagro.fr
³ Haute Ecole Province de Henaut—Condorcet, Rue Paul Pastur 11, 7800 Ath, Belgium; benoit.moreau@condorcet.be
* Correspondence: reinaldo.fraga@icidca.azcuba.cu; Tel.: +53-7-696-7015; Fax: +53-7-988243



Citation: Fraga Vidal, R.; Arísticas Ribalta, R.C.; Martínez Valdés, L.T.; Lafargue Gámez, M.; Montes Alvarez, A.; Rubio Sánchez, A.; Dubreucq, E.; Moreau, B. Construction of a Novel Chimeric Dextranucrase Fused to the Carbohydrate-Binding Module CBM2a. *Catalysts* **2021**, *11*, 1179. <https://doi.org/10.3390/catal11101179>

Academic Editor: Jose M. Guisan

Received: 30 August 2021

Accepted: 22 September 2021

Published: 28 September 2021

Publisher's Note: MDPI stays neutral with regard to jurisdictional claims in published maps and institutional affiliations.



Copyright: © 2021 by the authors. Licensee MDPI, Basel, Switzerland. This article is an open access article distributed under the terms and conditions of the Creative Commons Attribution (CC BY) license (<https://creativecommons.org/licenses/by/4.0/>).

Abstract: Lactic acid bacteria (LAB) have the potential to produce homoexopolysaccharides (HoPS). Their health benefits and physicochemical properties have been the subject of extensive research. The HoPS functional properties are determined by molecular weight, the type of glycosidic linkages, degrees of branching and chemical composition. The dextranases (DSases) produce a kind of HoPS (dextran), which are among the first biopolymers produced at industrial scale with applications in medicine and biotechnology. The glycodiversification opens additional applications for DSases. Therefore, the design and characterization of new DSases is of prime importance. Previously, we described the isolation and characterization of a novel extracellular dextranucrase (DSR-F) encoding gene. In this study, from DSR-F, we design a novel chimeric dextranucrase DSR-F-ΔSP-ΔGBD-CBM2a, where DSR-F-ΔSP-ΔGBD (APY repeats and a CW repeat deleted) was fused to the carbohydrate-binding module (CBM2a) of the β-1-4 exoglucanase/xylanase Cex (Xyn10A) of *Cellulomonas fimi* ATCC 484. This dextranucrase variant is active and the specificity is not altered. The DSR-F-ΔSP-ΔGBD-CBM2a was purified by cellulose affinity chromatography for the first time. This research showed that hybrids and chimeric biocatalyst DSases with novel binding capacity to cellulose can be designed to purify and immobilize using renewable lignocellulosic materials as supports.

Keywords: dextranases; GH70; lactic acid bacteria; sucrose-active enzymes; carbohydrate-binding module; glucanase; cellulose-binding domain; *Leuconostoc*

1. Introduction

Homoexopolysaccharides (HoPS) produced by lactic acid bacteria (LAB) have been the subject of much research to determine their physicochemical and bioactive properties [1]. The individual functional properties of HoPS are determined by their chemical composition, molecular weights, and types of glycosidic linkages as well as the degree and arrangement of branches [2]. The structural diversity of HoPS is a result of the unmatched variety of possible glycosidic bonds between sugar monomers, offering an extensive range of functionalities of interest for food, feed, pharmaceuticals, cosmetics and chemicals industries [3–6].

Dextran is among the first microbial HoPS produced at industrial scale [7]. Microorganisms of the genera *Lactobacillus*, *Streptococcus*, *Weissella* and *Leuconostoc* produce these polysaccharides [8]. The *Leuconostoc mesenteroides* NRRL B-512F is used for the synthesis of the most common commercial dextran. The biopolymer's main chain contains α(1-6)

linked glucosyl residues with only 5% of $\alpha(1-3)$ linked branches [7]. The dextran fractions of controlled molecular weight and their numerous derivatives are mainly used in medicine, pharmaceuticals and fine chemistry [9,10]. The extracellular glucansucrase (dextransucrase) DSR-S, a 6- α -D-glucosyltransferase (EC 2.4.1.5) is responsible for the polymer production [11]. This enzyme belongs to the glycoside hydrolase family 70 (GH70) according to the CAZy classification (<http://www.cazy.org/>) (accessed on 20 June 2021) [12]. The GH70 family consists of a large and diverse group of polymerases and branching enzymes, some of them being mainly active on sucrose while others typically use starch substrates [13,14].

The catalytic domain of GH70 presents the typical $(\alpha/\beta)_8$ barrel of glucansucrases. The three amino acids (D551, E589, D662, DSR-S numbering) forming the catalytic triad are highly conserved in the GH70 family [15–17].

The study of GH70 enzymes with different specificities from new LAB strains and from mining genome data sets could provide new insights into structure–function relationships of glucansucrases as well as enlarge the natural dextransucrase repertoire available for industrial application [18]. The Cuban Research Institute on Sugarcane By-products (ICIDCA) has a collection of LAB strains isolated from sugarcane and sugarcane derivatives. From those LAB strains, some dextransucrases have already been partially characterized [19–21]. From them, the DSR-F dextransucrase and its truncated variant DSR-F- Δ SP- Δ GBD have some common structural and functional characteristics with alternansucrase ASR. However, there are different specificities, as revealed by ^{13}C NMR spectra, which show dextran polymers formed by $\alpha(1-6)$ (93%), $\alpha(1-3)$ (6%) links, and $\alpha(1-4)$ (1%) branches [19,20]. In the present study, a chimeric dextransucrase from DSR-F- Δ SP- Δ GBD fused to the carbohydrate-binding module (CBM2a) of the exoglucanase/xylanase Cex (Xyn10A) of *Cellulomonas fimi* ATCC 484 was obtained. This variant, fully active, was purified by cellulose affinity chromatography and partially characterized. This chimeric dextransucrase could be purified or fractionated with sugarcane bagasse or bagasse derivatives but also immobilized in those types of renewable supports to produce maltooligosaccharides or modified oligodextrans with potential prebiotic properties.

2. Results and Discussion

2.1. Design of a Chimeric Dextransucrase (DSR-F- Δ SP- Δ GBD-CBM2a) Fused to the Carbohydrate-Binding Module CBM2a

Based on the 3D structural model of DSR-F- Δ SP- Δ GBD (Figure 1II), a chimeric dextransucrase fused to the carbohydrate-binding module CBM2a (DSR-F- Δ SP- Δ GBD-CBM2a) was constructed (Figure 1I,III). Deleting the two APY repeat units and a cell wall repeat unit (CW repeat) from the C-terminal end of DSR-F and adding the CBM2a allowed further investigation of this domain fusion on the specificity of the chimeric fused variant.

The recombinant DSR-F- Δ SP- Δ GBD enzyme produces a unique mostly linear $\alpha(1-6)$ (93%) dextran with minor branching $\alpha(1-3)$ (6%) and $\alpha(1-4)$ (1%) [19,20]. This enzyme variant was previously produced without part of its C-terminal glucan-binding domain (Figure 1I, DSR-F- Δ SP- Δ GBD). The deletion of the C-terminal domain V including the two APY repeats and a cell wall (CW) repeat did not affect the DSR-F- Δ SP- Δ GBD specificity and efficiency but increased its solubility during its expression and production in *E. coli*. [19]. Other examples of APY repeats that have been deleted without adverse effect on other GH70 and related enzymes have been observed in alternansucrase, inulosucrase, and branching sucrose BSR-B [22–24].

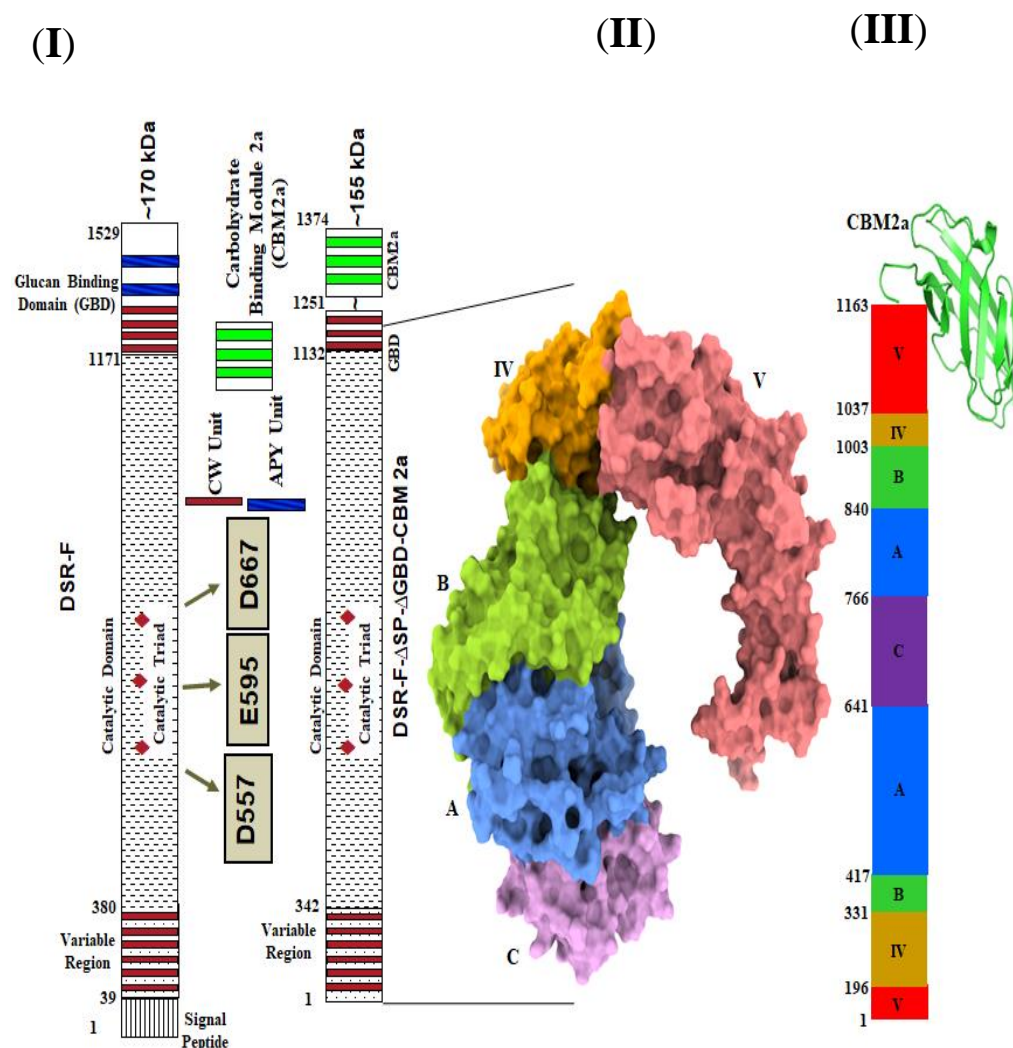


Figure 1. (I). Primary representation of dextransucrase DSR-F of *Leuconostoc citreum* B/110-1-2 and its deletion mutant DSRF-ΔSP-ΔGBD. (II). 3D structure model of DSRF-ΔSP-ΔGBD, five domains are highlighted, in red (domain V), yellow (domain IV), green (domain B), blue (domain A), and magenta (domain C). (III). Linear schematic representation of DSRF-ΔSP-ΔGBD domain organization with CBM2a fused to the C-terminal end.

2.2. Subcloning of DSR-F-ΔSP-ΔGBD to Obtain DSR-F-ΔSP-ΔGBD-CBM2a in the Expression Vector pdsrF-CBM2a and Purification of the Fusion Protein DSR-F-ΔSP-ΔGBD-CBM2a

The construction of plasmid pdsrF-CBM2a allows the inducible expression of DsrF-ΔSP-ΔGBD fused in its carboxyl end region with the carbohydrate-binding module CBM2a of Cex, a β -1,4-exo-glucanase of *Cellulomonas fimi* ATCC 484. The fusion of the CBM2a to a dextransucrase is reported for the first time. The presence of the CBM2a module seems to not affect the ability to form dextran polymer by the fusion enzyme DsrF-ΔSP-ΔGBD-CBM2a (Figure 2I,II), and it will permit its purification for further characterization and future immobilization on cellulosic or lignocellulosic materials. A successful dextransucrase fusion for immobilization is the case of DSR-S from *Leuconostoc mesenteroides* B-512FMC to glutathione S-transferase (GST), resulting in a novel and completely active fused truncated variant [25].

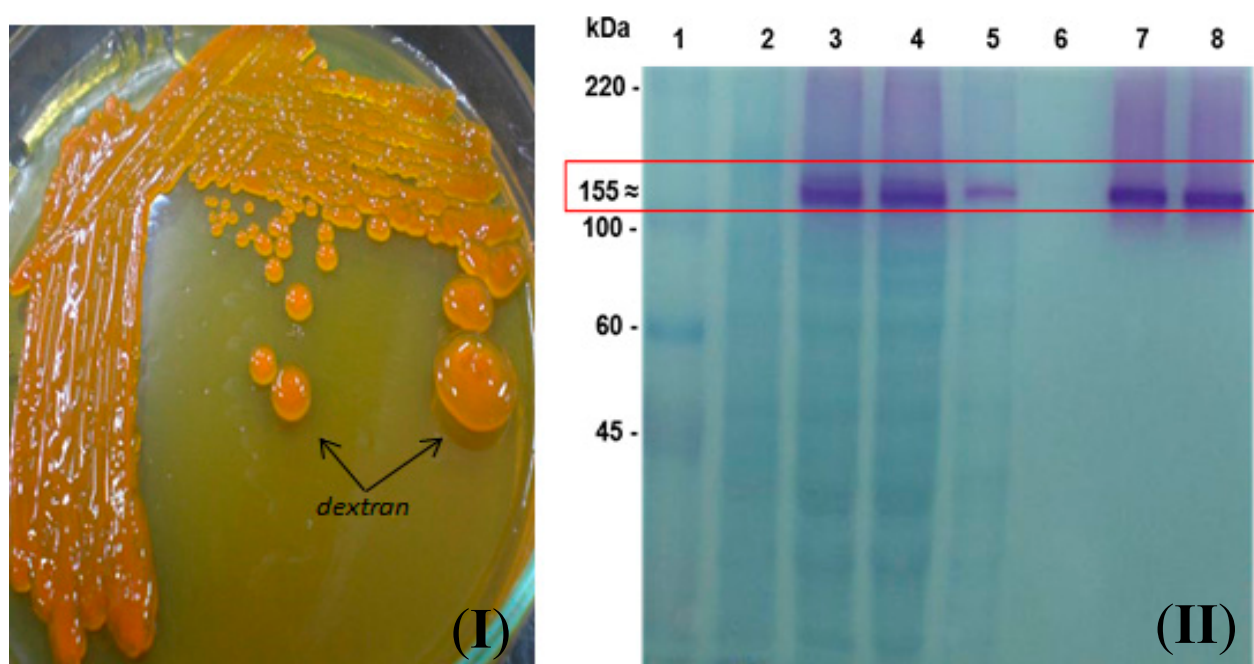


Figure 2. Production of DsrF-ΔSP-ΔGBD-CBM2a in *E. coli* DH10B. (I) Detection of dextranase activity through the formation of dextran on LBT agar plate. (II) SDS-PAGE of DsrF-ΔSP-ΔGBD-CBM2a purification, stained combining two detection methods. Zymography of the proteins with dextranase activity (colored bands), followed by detection of total proteins by negative staining with imidazole and zinc sulfate salts (transparent bands). The formation of the dextran polymer demonstrates the activity of the fusion. (1) Molecular Weight Marker (ColorBurst™, Sigma-Aldrich Co.). (2) Soluble fraction of *E. coli* DH10B (pSE380) cell lysate as negative control. (3) Soluble fraction of *E. coli* DH10B (pdsrF-CBD) cell lysate. (4) Flowthrough fraction, not retained by the RAC. (5) Fraction of the 1st wash of the column (8 Column Volumes, CV). (6) Fraction of the 2nd wash of the column (12 CV). (7 and 8) Fractions eluted.

The purification of DsrF-ΔSP-ΔGBD-CBM2a from the soluble fraction of the *E. coli* DH10B (pdsrF-CBM2a) was performed using regenerated amorphous cellulose (RAC) as an affinity resin. The purified protein migrated as a single band with an apparent molecular mass of 155 kDa and a 90–95% purity estimated by densitometry (Figure 2II). This is the first report of the use of a cellulose-based matrix for the purification of a dextranase by affinity chromatography. The levels of purified protein are greater than those achieved by the immobilized metal ion affinity chromatography (IMAC) (data not shown). This may be because RAC has a higher binding capacity (365 mg of protein per gram of RAC) than any other commercial resin used to purify proteins (10–40 mg of proteins per gram of resin) [26]. However, the purification conditions tested were not optimized, explaining why a lot of enzyme was not retained by the cellulose resin. Changing some purification parameters such as the ratio of crude extract protein to resin would improve the procedure.

2.3. Action of DSR-F-ΔSP-ΔGBD-CBM2a in Polymerization and Acceptor Reactions

A polymerization reaction with sucrose was carried out to ensure the chimeric DSR-F-ΔSP-ΔGBD-CBM2a behaves in the same way as the DSR-F-ΔSP-ΔGBD variant. Dextranase GTF180 from *Lb. reuteri* 180 [27] and alternansucrase (ASR) from *L. citreum* NRRL B-1355 [28], DSR-F-ΔSP-ΔGBD-CBM2a and DSR-F-ΔSP-ΔGBD are also striking examples of α -transglucosylases among GH70 glucansucrases. They catalyze a bi-modal population of glucan, comprising a high-molar mass (HMM, 2×10^6 g·mol^{−1}) dextran and low-molar mass gluco-oligosaccharides (LMM, DP < 8, around 1300 g·mol^{−1}) from sucrose, as estimated by size exclusion chromatography (Figure 3I).

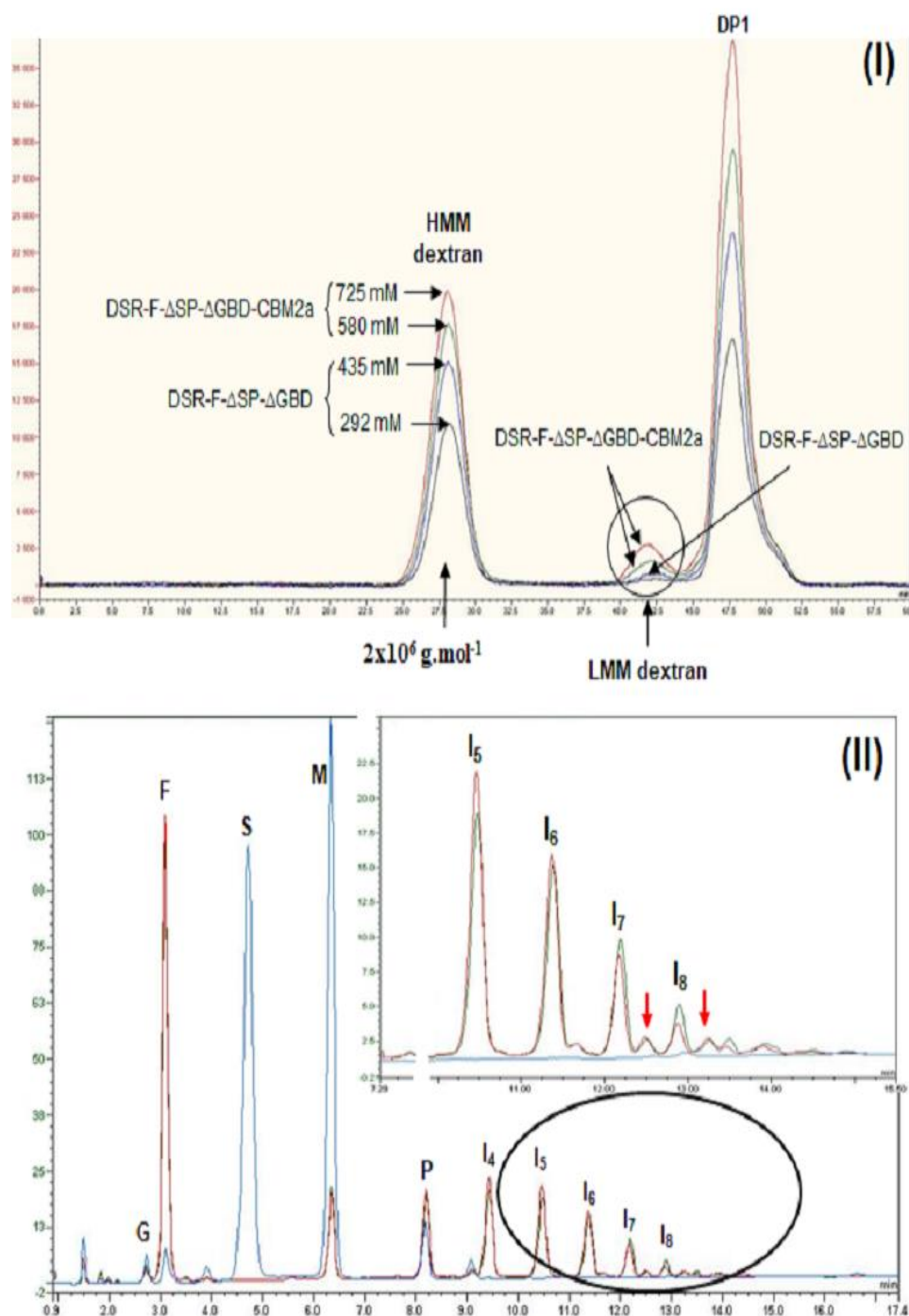


Figure 3. (I) Analysis of HPSEC chromatograms synthesized using the chimeric dextran sucrose DSR-F- Δ SP- Δ GBD-CBM2a (from 580 and 725 mM sucrose) and DSR-F- Δ SP- Δ GBD (from 292 and 435 mM sucrose) with 50 mM sodium acetate buffer, pH 5.5 and $1 \text{ U} \cdot \text{mL}^{-1}$ enzyme. Enzymatic reactions were stopped after 24 h. Peak identification: HMM dextran—high-molecular mass dextran ($2 \times 10^6 \text{ g} \cdot \text{mol}^{-1}$ as estimated by HPSEC), LMM dextran—low-molecular mass dextran (oligosaccharides of DP <8), DP1—fructose. (II) Analysis of HPAEC-PAD chromatogram products synthesized using DSR-F- Δ SP- Δ GBD-CBM2a (green line) and DSR-F- Δ SP- Δ GBD (red line) from sucrose (292 mM) and maltose (146 mM) with 20 mM sodium acetate buffer, pH 5.5 and $1 \text{ U} \cdot \text{mL}^{-1}$ enzyme. Enzymatic reactions were stopped after 24 h. Arrows indicate extra peaks after products with degrees of polymerization (DP) of 7 and 8. Peak identification: G—glucose, F—fructose, S—sucrose, M—maltose, P—panose (DP3), I₄–I₈—isomaltooligosaccharides of DP4–DP8. The line with the highest signal of S and M and no detection of isomaltooligosaccharides corresponds to the initial reaction time ($t = 0 \text{ min}$, blue line).

This result corroborates the dextran formation observed in Figure 2I,II. In addition, it suggests a semi-processive elongation mechanism, as for other GH70 enzymes, where smaller oligosaccharides are produced in a non-processive mode at the beginning of the reaction. When a critical length is reached, a processive mechanism, mediated by polymer-binding regions in the enzyme, starts, helped by the glucan-binding domain to facilitate HMM dextran formation [29,30]. The horseshoe shaped putative structure of DSR-F- Δ SP- Δ GBD-CBM2a and DSR-F- Δ SP- Δ GBD (Figure 1II) could give high flexibility to domain V like in others GH70, which in combination with several putative binding pockets identified (Figure 4I,II) could promote a local increase in dextran concentration around the catalytic site for chain elongation.

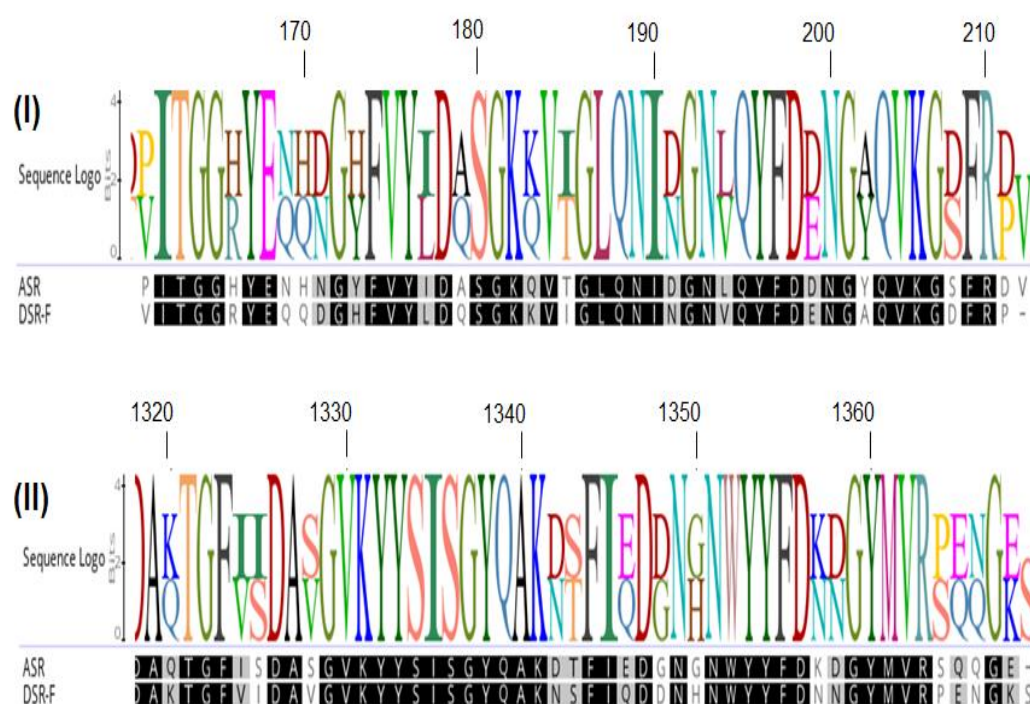


Figure 4. Domain V sugar-binding pockets sequence comparison. Alignment of the residues corresponding to two sugar-binding pockets V-A (I) and V-C (II) of alternansucrase ASR from *L. citreum* NRRL B-1355 (PDB entry 6SYQ) with the equivalent residues in dextranase DSR-F.

In the acceptor reaction (maltose as the acceptor molecule) performed with DSR-F- Δ SP- Δ GBD-CBM2a, a series of analog isomaltodextrins very similar to the ones produced by the recombinant dextranase DSR-F- Δ SP- Δ GBD from *L. citreum* B/110-1-2 (Figure 3II) were synthesized. The isomalto-oligosaccharide (IMO) products with 7 and 8 glucose units showed two extra peaks (Figure 3II, arrows), indicating that they were decorated with at least one branched α (1–4) glucose unit. These IMO products correspond to previously characterized oligodextrins [20]. From these observations, it seems that the cellulose-binding domain of DSR-F- Δ SP- Δ GBD-CBM2a does not affect the synthesis of HMM and LMM glucans from sucrose and IMO products from sucrose/maltose, respectively.

2.4. Action of DSR-F- Δ SP- Δ GBD-CBM2a from Sucrose and Linear Oligodextrans (1500 and 6000 g·mol^{−1})

A reaction with sucrose (292 mM), 1500 g·mol^{−1} dextran (66.6 mM), a linear α (1–6) glucan with a mean DP of 9 was performed. Analyses of the reaction products showed that a low amount of leucrose was detected due to the action of fructose as an acceptor (Figure 5IB,C). This kind of transglycosylation has been reported to be favored at the start of the dextran sucrose reactions [29,31]. It has been recently suggested that leucrose acts as the substrate for further dextran formation or elongation of IMOs [32]. The IMOs from DP8 to DP12 were glucosyl decorated in the same way by the chimeric dextran sucrose DSR-F- Δ SP- Δ GBD-CBM2a and DSR-F- Δ SP- Δ GBD, leading to the formation of products clearly observable on HPAEC-PAD chromatograms (Figure 5IB,C, arrows). Such chromatographic patterns resulting from the acceptor reaction (oligodextrans as the acceptor molecules) is reported for the first time for a DSR-F variant enzyme. According to the specificity of both analyzed enzymes, these modified IMOs could be products partially glucosylated and likely altered by addition of α (1–4) branched glucose units. As a specific population of IMOs seems to act as acceptor molecules to be branched, two factors could be involved with this observation. Structural analyses of dextrans have identified a relation between the degree of branching and the rms charge radii of the polymers wherein a higher proportion of more branched and more compact dextrans is formed. On the other hand, branching may also depend on the steric properties of the glucosyl-donor in the active site of the enzyme [32]. However, the structure of these products (DP8–DP12) must be elucidated in more detail.

A reaction using sucrose (292 mM) and 6000 g·mol^{−1} dextran (66.6 mM), a linear α (1–6) glucan or oligodextran with a mean degree of polymerization of 37 was performed. As seen on the HPAEC-PAD chromatograms, the product profile after a 24 h reaction was different from the initial reaction profile. As in the previous reaction, a low amount of leucrose was detected. Analyses of the final reaction products showed the intensity of several peaks corresponding to isomaltooligosaccharides decreased, suggesting those products were modified in a similar way by DSR-F- Δ SP- Δ GBD-CBM2a and DSR-F- Δ SP- Δ GBD enzymes (Figure 5IIB,C, arrows). The depletion of all low-molecular weight oligosaccharides suggests such molecules are acting as glucosyl acceptors and are further elongated, probably because in both enzymes some kind of interaction with IMOs are taking place. Recently, the first functional surface binding site (SBS-A1) for a GH70 family enzyme (ASR) was described. It binds isomaltose, isomaltotriose, isomaltotetraose, panose and oligoaltetran [30]. An alignment sequence of SBS-A1 and the equivalent residues in dextran sucrose DSR-F is shown in Figure 6. Several residues are highly conserved in both sequences which could be associated with a similar functionality in DSR-F. From the product analysis of the reactions performed in this study, it seems that dextran sucrose DSR-F variants show a strong transferase activity since sucrose was completely consumed and the contents of free glucose and leucrose seem to be much lower than fructose. Therefore, further studies are needed to corroborate a potential utilization of short IMOs as glucosyl acceptors during dextran synthesis and dextran modifications by dextran sucrose- α -transglucosylases enzymes.

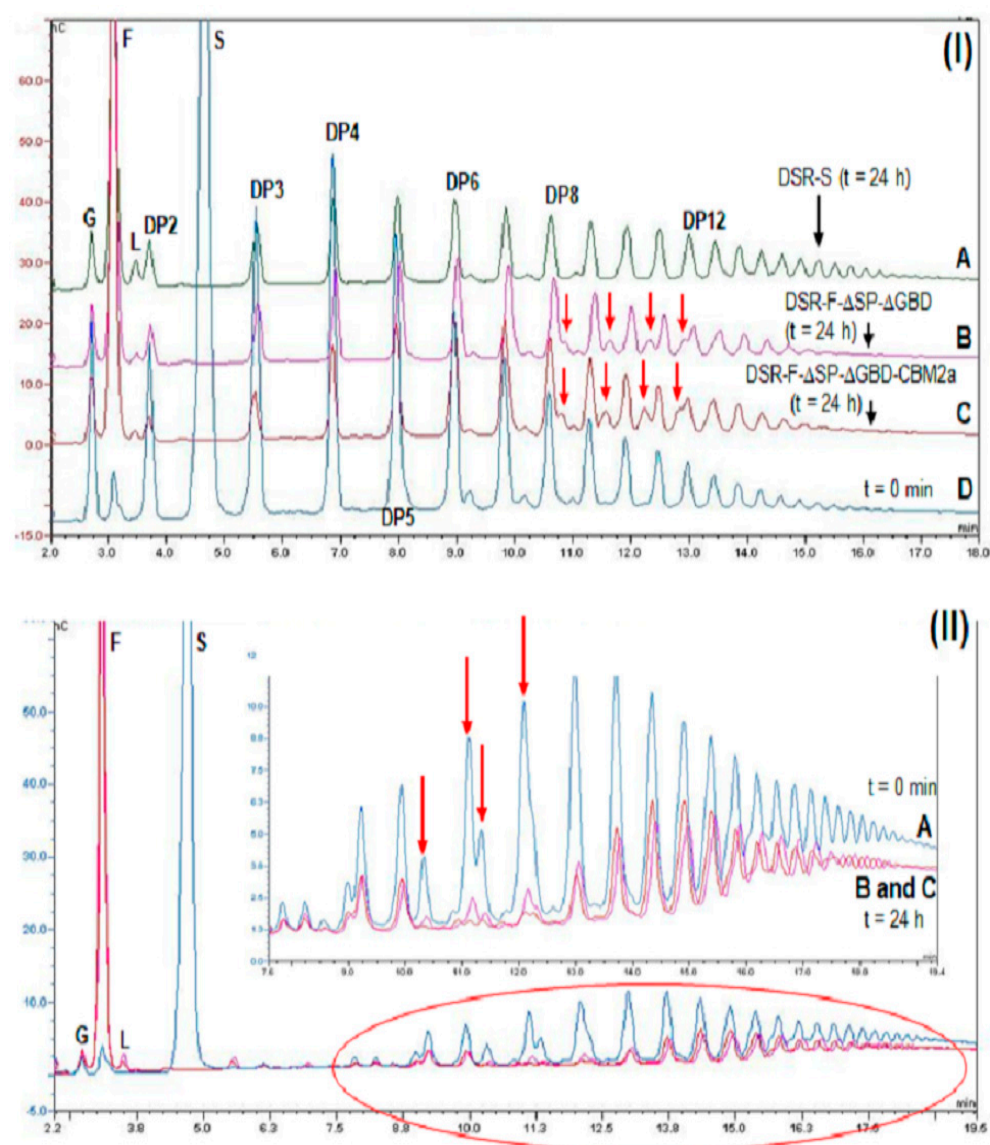


Figure 5. (I) Analysis of HPAEC-PAD chromatogram products synthesized using the chimeric dextranase DSR-F-ΔSP-ΔGBD-CBM2a, DSR-F-ΔSP-ΔGBD and native dextranase DSR-S from *Leuconostoc mesenteroides* NRRL B-512F from sucrose (292 mM) and dextran 1500 g·mol^{−1} (66.6 mM) with 20 mM sodium acetate buffer, pH 5.5 and 1 U·mL^{−1} enzyme. Enzymatic reactions were stopped after 24 h, nC, (nanocoulombs). I-(A) Enzymatic reaction using DSR-S from *L. mesenteroides* NRRL-B512; I-(B) enzymatic reaction using DSR-F-ΔSP-ΔGBD recombinant; I-(C) enzymatic reaction using chimeric dextranase DSR-F-ΔSP-ΔGBD-CBM2a; I-(D) enzymatic reaction using chimeric dextranase DSR-F-ΔSP-ΔGBD-CBM2a at the initial time (t = 0 min). Arrows indicate four extra peaks immediately after the products with degrees of polymerization (DP) of 8–12, respectively. (II) Analysis of HPAEC-PAD chromatogram products synthesized using the chimeric dextranase DSR-F-ΔSP-ΔGBD-CBM2a and DSR-F-ΔSP-ΔGBD sucrose (292 mM) and 6000 g·mol^{−1} dextran (66.6 mM) with 20 mM sodium acetate buffer, pH 5.5 and 1 U·mL^{−1} enzyme. Enzymatic reactions were stopped after 24 h. II-(A) Enzymatic reaction using chimeric dextranase DSR-F-ΔSP-ΔGBD-CBM2a at the initial time (t = 0 min); II-(B) and II-(C) enzymatic reaction using DSR-F-ΔSP-ΔGBD-CBM2a and DSR-F-ΔSP-ΔGBD, respectively. Arrows indicate peaks corresponding to modified dextrans from the initial reaction time. Peak identification: G—glucose, F—fructose, L—leucrose, S—sucrose, DP2–DP12—isomaltooligosaccharides with a degree of polymerization (DP) from 2 to 12.

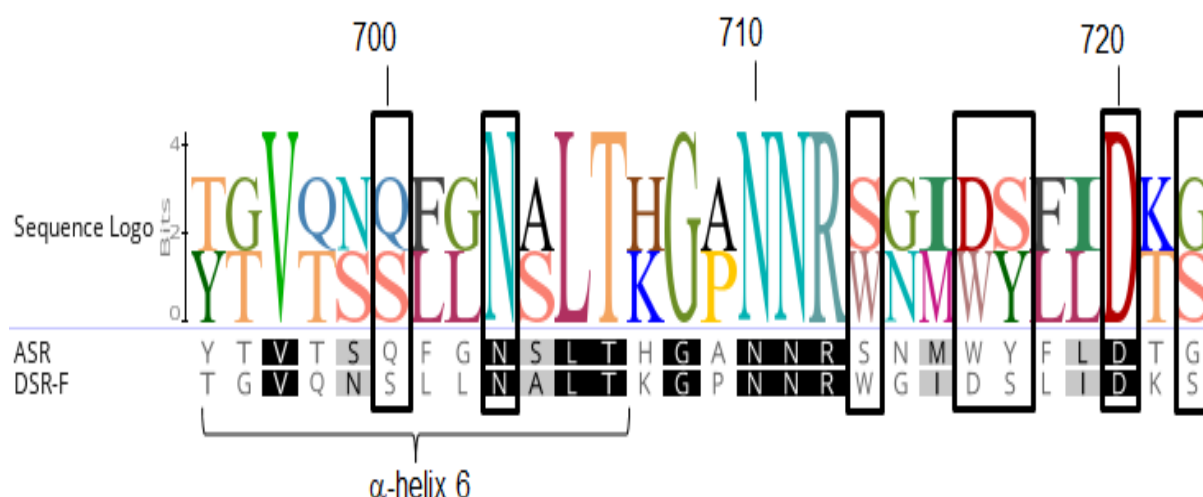


Figure 6. Surface binding site (SBS-A1) sequence comparison. Alignment of the residues corresponding to SBS-A1 of alternansucrase ASR (in black boxes) from *L. citreum* NRRL B-1355 (numbered and α -helix 6 according to ASR in complex with isomaltotriose, PDB entry 6SYQ) with the equivalent residues in dextranucrase DSR-F.

3. Materials and Methods

3.1. Bacterial Strains and Culture Media

Escherichia coli DH10B was used for the subcloning steps and for protein expression with the pSE380 vector (Invitrogen, Waltham, MA, USA). The screening of *E. coli* colonies producing functional dextranucrase enzymes was carried out using LBT agar medium [11,20]. Briefly, LBT agar was supplemented with the pH indicator bromothymol blue (0.025%) (Sigma, Saint Louis, MO, USA), 5% sucrose (Sigma, USA) and 1% glycerol as extra carbon sources, IPTG (0.08%) (Sigma, USA), ampicillin ($100 \mu\text{g mL}^{-1}$) (Sigma, USA). *E. coli* was grown and maintained on LB medium supplemented when needed with ampicillin ($100 \mu\text{g mL}^{-1}$). All strains were stored at -80°C in 15% glycerol.

3.2. Subcloning to Express the *dsrF*- Δ SP- Δ GBD-CBM2a Gene in *E. coli*

All plasmids for the subcloning steps are listed in Table 1. The 3.7 kb fragment encoding the truncated variant of DsrF (DsrF- Δ SP- Δ GBD) was digested with the restriction enzymes *NcoI*-*EcoRI* from the pSEdsrF plasmid and inserted into the plasmid pET38b (+) (Novagen, Madison, WI, USA), which was also digested with the same restriction enzymes, to create the 9.5 kb pETdsrF plasmid (Km^r) after the ligation of both fragments. The latter contains the truncated variant dsrF- Δ SP- Δ GBD under the inducible promoter PT7lac, fused at the 3' end to the signal peptide of the exo- β -1,4-glucanase Cex from *Cellulomonas fimi* ATCC 484, at the 5' end of the cellulose-binding module (CBM2a) of said enzyme, and to the His₈ tag. Likewise, the truncated variant is also fused to the 5'-terminus of the transcription terminator of bacteriophage T7. The strain of *E. coli* DH10B was transformed with the plasmid pETdsrF, which was subsequently purified and digested with the restriction enzymes *NcoI*-*AvrII* releasing the *dsrF*- Δ SP- Δ GBD fused with the CBM2a and the His₈ tag. This fragment was ligated to the equally digested pSE380 plasmid *NcoI*-*AvrII*, giving rise to the 8.4 kb pdsrF-CBM2a plasmid (Ap^r) containing the *dsrF*- Δ SP- Δ GBD-CBM2a fragment under the inducible P_{trc} promoter, fused at the end 3' to the terminator of the transcription of *E. coli* rrnBt1-t2. The strain of *E. coli* DH10B was transformed with this plasmid.

Table 1. Plasmids used in this work.

| Plasmids | Description | Reference |
|-------------|---|------------|
| pET38b(+) | Replicon <i>colE1</i> , vector used for protein production in <i>E. coli</i> , fused to the signal secretion Cex downstream the PT7lac promoter. It harbours the encoding region for the Carbohydrate-Binding Module. (CBM2a) and a His ₈ tag, Km ^r , size: 5.8 kb. | Novagen |
| pSE380 | Replicon <i>colE1</i> , vector used for protein production in <i>E. coli</i> downstream the PTrc promoter, Ap ^r , size: 4.4 kb. | Invitrogen |
| pSEdsrF | pSE380 <i>NcoI-EcoRI</i> , fused to the 3.7 kb amplicon <i>NcoI-EcoRI</i> obtained from pGEMdsrF. Harbours the truncated variant DsrF-ΔSP-ΔGBD, Ap ^r , size: 8.1 kb | [19] |
| pETdsrF | pET38b(+) <i>NcoI-EcoRI</i> , fused to the 3.7 kb (DsrF-ΔSP-ΔGBD) <i>NcoI-EcoRI</i> from pSEdsrF, Km ^r , size: 9.5 kb. | This work |
| pdsrF-CBM2a | pSE380 <i>NcoI-AvrII</i> , fused to the 4.2 kb DNA fragment (DsrF-ΔSP-ΔGBD-CBM2a) <i>NcoI-AvrII</i> from pETdsrF, Ap ^r , size: 8.6 kb. | This work |

3.3. Inducible Production of DSR-F-ΔSP-ΔGBD-CBM2a in *E. coli*

For the production of the recombinant dextranucrase DsrF-ΔSP-ΔGBD-CBM2a, a colony of the recombinant strain of *E. coli* DH10B (pdsrF-CBM2a) was inoculated in 100 mL invaginated flasks with 10 mL of 2xYT medium supplemented with 100 mM Tris/HCl, pH 6.4, 100 µg·mL⁻¹ ampicillin at 30 °C, and grown overnight at 175 r·min⁻¹. The next day, the cultures were diluted 1:100 with the same medium, supplemented with ampicillin 200 µg·mL⁻¹ and grown at 30 °C to an OD (600 nm) 0.5 with shaking at 175 r·min⁻¹. Isopropyl-1-thio-β-D-galactopyranoside (IPTG) (inducer of the P_{trc} promoter) was added at a final concentration of 2.4 mmol·L⁻¹ and incubated for 12–14 h at 20 °C with shaking at 175 r·min⁻¹. The cells were collected by centrifugation (Eppendorf 5804 R centrifuge) at 10,000 × *g* for 15 min at 4 °C and resuspended in the rupture buffer (50 mM NaAc, pH 5.4, Triton X 100 0.1% (*v/v*), CaCl₂ 0.05 g·L⁻¹, cocktail of protease inhibitors (Roche)) up to an OD (600 nm) of 80. Cell disruption was performed by ultrasound in a disruptor (MSP, Berks, England). The sample (always kept on ice) was exposed to seven cycles of 1 min, at a constant amplitude of 28 microns, with one minute of rest between cycles. The lysate extract was centrifuged (Eppendorf 5804 R centrifuge) at 21,390 × *g* for 40 min, and the soluble and insoluble fraction of each cell extract was recovered. The samples were stored at −20 °C until they were used in other analyses.

3.4. Cellulose Affinity Chromatography (CAC)

The chimeric DSR-F-ΔSP-ΔGBD-CBM2a was purified by cellulose affinity chromatography (CAC). For this, a matrix of regenerated amorphous cellulose (RAC) obtained from Microgranular Cellulose CC31 (Whatman, Florham Park, NJ, USA) was used [33]. The soluble fraction of the sonicate extract (10 mL) was mixed by slow agitation with 5 mL of RAC for 2 h at 4 °C. The enzyme bound to the matrix was recovered by centrifugation (Eppendorf 5804 R, Hamburg, Germany) at 3500 × *g* for 5 min and packed in a 10 mL column (10 cm × 2 cm Ø). The protein was eluted with 10 mL of glycerol 99%.

3.5. Determination of Enzymatic Activity Dextranucrase

The enzymatic activity assay was performed at 30 and 40 °C, in 20 mM sodium acetate buffer (pH 5.4), 0.05 g·L⁻¹ CaCl₂, 1 g·L⁻¹ NaN₃, and 100 g·L⁻¹ sucrose. The saccharolytic activity was determined by detecting the levels of free reducing sugars with the dinitrosalicylic acid (DNSA) method [34]. One unit of activity was defined as the amount of enzyme that catalyzed the release of 1 µmol·min⁻¹ of fructose under the conditions tested. The concentration of proteins was determined according to [35] using BSA as a standard. All determinations were made in triplicate.

3.6. SDS-PAGE and Zymograms

Protein electrophoresis under denaturing conditions (SDS-PAGE) was performed with the XCell SureLock™ Mini-Cell system, with NOVEX Tris–Acetate gels of 1.5 mm thickness, NuPAGE® antioxidant and NuPAGE® Tris–Acetate SDS Running Buffer (for Tris–Acetate gels) from Invitrogen. The NuPAGE® Sample Reducing Agent (3 mL) and NuPAGE® LDS Sample Buffer (X4) (7.5 mL) were mixed with 20 µL of sample and heated at 70 °C for 10 min prior to being loaded onto gels. Samples containing suspended cells were centrifuged at $10,000 \times g$ in a micro-centrifuge before being applied to the gels. Approximately 2 mU of enzyme was loaded onto the gels and electrophoresis was carried out for 1 h at 150 V. The gels were stained for dextranucrase activity in situ (based on Schiff's reaction) according to the procedure of [36] in combination with a reversible negative protein staining method [37]. Briefly, after Schiff's staining, the gel was soaked in a solution (~50 mL) of Imidazole-SDS (20 mM and 0.1%, respectively) for 30 min. This solution was discarded, ~30 mL of ZnSO₄ 20 mM was added, and shaken by hand on a dark surface until the protein bands became visible. To stop this reaction, the solution was discarded and the gel was washed several times with deionized water. Precision Plus Protein™ All Blue Standard was included in all electrophoresis runs.

3.7. Production of High-Molecular Weight Dextrans, Maltooligosaccharides, and Linear Dextran Modification

High-molecular-weight dextran synthesis was performed at 40 °C for 24 h, in buffer 20 mM NaAc (pH 5.4), 0.05 g·L^{−1} CaCl₂, 1 g·L^{−1} NaN₃, 100 g·L^{−1} sucrose and 1 U·mL^{−1} enzyme. Maltooligosaccharides were produced under the same conditions, except maltose 50 g·L^{−1} was added to the reaction. Linear dextrans were modified under the same conditions but 66.6 mM of α-1,6 dextrans (1500 g·mol^{−1} and 6000 g·mol^{−1}; Sigma, USA) were added.

3.8. High-Performance Anion-Exchange Chromatography with Pulsed Amperometric Detection (HPAEC-PAD)

Synthesized oligosaccharides were analyzed by high HPAEC-PAD using a Dionex CarboPac PA100 (ThermoFisher, Barcelona, Spain) 4 × 250 mm column at room temperature. A gradient of sodium acetate (from 6 to 300 mM in 28 min) was applied in 150 mM NaOH at a flow rate of 1 mL·min^{−1}. Detection was performed with an ED40 Dionex module gold electrode and a reference electrode pH Ag/AgCl. Standards used were glucose, fructose, sucrose, panose, and leucrose, prepared as 10 mg·mL^{−1} in buffer 20 mM NaAc (pH 5.4). The samples were diluted 10 times in water and were filtered through membranes with pores of 0.20 µm (Sartorius) before injection.

3.9. High-Performance Size Exclusion Chromatography (HPSEC)

Dextran molecular weights were determined by HPSEC. Two Shodex OH-Pack SB-805 and SB-802.5 columns were maintained in series, using an eluent containing 0.45 M of NaN₃ and 1% of ethylene glycol at a flow rate of 0.3 mL min^{−1}. Columns and guard columns were maintained at 70 °C, and samples were filtered through a 0.45 µm-pore-size filter (Sartorius) before injection [29]. The reaction was stopped after 24 h by heating for 5 min at 95 °C in a boiling water bath. Calibration standards of commercial dextrans of 2×10^6 g·mol^{−1}, 530,103 g·mol^{−1}, 70×10^3 g·mol^{−1}, and 10×10^3 g·mol^{−1} (Sigma-Aldrich) were used.

4. Conclusions

Both enzymes were able to produce HMM and LMM polymers from sucrose, and isomaltooligosaccharides from sucrose/maltose. They were also able to modify at least two kinds of linear dextrans (1500 and 6000 g·mol^{−1}), making the DSR-F-ΔSP-ΔGBD-CBM2a and DSR-F-ΔSP-ΔGBD biocatalysts act as efficient α-transglucosidases in the presence of sucrose and linear oligodextrans. The additional cellulose-binding domain of the fusion

enzyme does not affect the modification capacity on linear oligodextrans. Investigation of the relationship between structure and function of DSR-F variants will undoubtedly improve understanding of the polymerization mechanism of this enzyme and of GH70 glucansucrases in general. Considering its specificity, this fusion variant holds great potential for the production of novel functional foods.

Author Contributions: Conceptualization, R.F.V. and R.C.A.R.; methodology, L.T.M.V.; software, R.F.V. and E.D.; validation, M.L.G., A.M.A. and A.R.S.; formal analysis, R.F.V.; investigation, R.F.V., M.L.G., A.M.A. and A.R.S.; resources, E.D.; data curation, R.F.V.; writing—original draft preparation, R.F.V.; writing—review and editing, R.F.V.; supervision, E.D.; project administration, B.M.; funding acquisition, B.M. All authors have read and agreed to the published version of the manuscript.

Funding: This research and the ACP were funded by Development Research Project financed by the Development Cooperation Program of ARES (Académie de Recherche et d’Enseignement Supérieur) from Belgium (2017–2022).

Acknowledgments: Reinaldo Fraga Vidal and Roberto C. Aríticas Ribalta were supported by a Development Research Project financed by the Development Cooperation Program of ARES (Académie de Recherche et d’Enseignement Supérieur) from Belgium (2017–2022). Reinaldo Fraga Vidal thanks William David Rau (MS Rau Antiques, New Orleans, LA, USA) for his kind support. We thank Magali Remaud-Simeon and Pierre Monsan for their technical support. We also thank Joan Combie for the style correction of the manuscript.

Conflicts of Interest: The authors declare no conflict of interest. The funders had no role in the design of the study; in the collection, analyses, or interpretation of data; in the writing of the manuscript, or in the decision to publish the results.

References

1. Pu, Y.; Zou, Q.; Hou, D.; Zhang, Y.; Chen, S. Molecular weight kinetics and chain scission models for dextran polymers during ultrasonic degradation. *Carbohydr. Polym.* **2017**, *156*, 71–76. [\[CrossRef\]](#) [\[PubMed\]](#)
2. Zannini, E.; Waters, D.M.; Coffey, A.; Arendt, E.K. Production, properties, and industrial food application of lactic acid bacteria-derived exopolysaccharides. *Appl. Microbiol. Biotechnol.* **2016**, *100*, 1121–1135. [\[CrossRef\]](#)
3. Vettori, M.H.P.B.; Blanco, K.C.; Cortez, M.; De Lima, C.J.B.; Contiero, J. Dextran: Effect of process parameters on production, purification and molecular weight and recent applications. *Diálogos Cienc.* **2012**, 171–186. [\[CrossRef\]](#)
4. Ryan, P.M.; Ross, R.P.; Fitzgerald, G.F.; Caplice, N.M.; Stanton, C. Sugar-coated: Exopolysaccharide producing lactic acid bacteria for food and human health applications. *Food Funct.* **2015**, *6*, 679–693. [\[CrossRef\]](#) [\[PubMed\]](#)
5. Salazar, N.; Gueimonde, M.; De Los Reyes-Gavilán, C.G.; Ruas-Madiedo, P. Exopolysaccharides Produced by Lactic Acid Bacteria and Bifidobacteria as Fermentable Substrates by the Intestinal Microbiota. *Crit. Rev. Food Sci. Nutr.* **2016**, *56*, 1440–1453. [\[CrossRef\]](#) [\[PubMed\]](#)
6. Xu, L.; Zhang, J. Bacterial glucans: Production, properties, and applications. *Appl. Microbiol. Biotechnol.* **2016**, *100*, 9023–9036. [\[CrossRef\]](#) [\[PubMed\]](#)
7. Naessens, M.; Cerdobek, A.; Soetaert, W.; Vandamme, E.J. *Leuconostoc* dextranase and dextran: Production, properties and applications. *J. Chem. Technol. Biotechnol.* **2005**, *80*, 845–860. [\[CrossRef\]](#)
8. Chen, Z.; Ni, D.; Zhang, W.; Stressler, T.; Mu, W. Lactic acid bacteria-derived α -glucans: From enzymatic synthesis to miscellaneous applications. *Biotechnol. Adv.* **2021**, *47*, 107708. [\[CrossRef\]](#)
9. Badel, S.; Bernardi, T.; Michaud, P. New perspectives for Lactobacilli exopolysaccharides. *Biotechnol. Adv.* **2011**, *29*, 54–66. [\[CrossRef\]](#)
10. Zdolsek, H.J.; Vegfors, M.; Lindahl, T.L.; Tornquist, T.; Bortnik, P.; Hahn, R.G. Hydroxyethyl starches and dextran during hip replacement surgery: Effects on blood volume and coagulation. *Acta Anaesthesiol. Scand.* **2011**, *55*, 677–685. [\[CrossRef\]](#)
11. Monchois, V.; Remaud-Simeon, M.; Russel, R.R.; Monsan, P.; Willemot, R.M. Characterization of *Leuconostoc mesenteroides* NRRL B-512F dextranase (DSRs) and identification of amino-acid residues playing a key role in enzyme activity. *Appl. Microbiol. Biotechnol.* **1997**, *48*, 465–472. [\[CrossRef\]](#) [\[PubMed\]](#)
12. Lombard, V.; Golaconda Ramulu, H.; Drula, E.; Coutinho, P.M.; Henrissat, B. The Carbohydrate-active enzymes database (CAZy) in 2013. *Nucleic Acids Res.* **2014**, *42*, D490–D495. [\[CrossRef\]](#) [\[PubMed\]](#)
13. Passerini, D.; Vuillemin, M.; Ufarté, L.; Morel, S.; Loux, V.; Fontagné-Faucher, C.; Monsan, P.; Remaud-Siméon, M.; Moulis, C. Inventory of the GH70 enzymes encoded by *Leuconostoc citreum* NRRL B-1299—identification of three novel-transglucosylases. *FEBS J.* **2015**, *282*, 2115–2130. [\[CrossRef\]](#) [\[PubMed\]](#)
14. Gangoiti, J.; van Leeuwen, S.; Gerwig, G.; Duboux, S.; Vafiadi, C.; Pijning, T.; Dijkhuizen, L. 4,3- α -Glucanotransferase, a novel reaction specificity in glycoside hydrolase family 70 and clan GH-H. *Sci. Rep.* **2017**, *7*, 39761. [\[CrossRef\]](#)

15. Macgregor, E.A.; Jespersen, H.M.; Svensson, B. A circularly permuted alpha-amylase-type alpha/beta-barrel structure in glucan-synthesizing glucosyltransferases. *FEBS Lett.* **1996**, *378*, 263–266. [\[CrossRef\]](#)
16. Vujčić-Zagar, A.; Dijkstra, B.W. Monoclinic crystal form of *Aspergillus niger* alpha-amylase in complex with maltose at 1.8 angstroms resolution. *Acta Crystallogr. Sect. F Struct. Biol. Cryst. Commun.* **2006**, *62*, 716–721. [\[CrossRef\]](#)
17. Pijning, T.; Vujčić-Zagar, A.; Kralj, S.; Eeuwema, W.; Dijkhuizen, L.; Dijkstra, B.W. Biochemical and crystallographic characterization of a glucansucrase from *Lactobacillus reuteri* 180. *Biotrans.* **2008**, *26*, 12–17. [\[CrossRef\]](#)
18. Molina, M.; Cioci, G.; Moulis, C.; Séverac, E.; Remaud-Simeon, M. Bacterial α -Glucan and branching sucraes from GH70 Family: Discovery, structure-function relationship studies and engineering. *Microorganisms* **2021**, *9*, 1607. [\[CrossRef\]](#)
19. Fraga, R.; Moulis, C.; Escalier, P.; Remaud-Simeón, M.; Monsan, P. Isolation of a Gene from *Leuconostoc citreum* B/110-1-2 Encoding a Novel Dextransucrase Enzyme. *Curr. Microbiol.* **2011**, *62*, 1260–1266. [\[CrossRef\]](#)
20. Fraga, R.; Martínez, A.; Moulis, C.; Escalier, P.; Morel, S.; Remaud-Siméon, M.; Monsan, P. A novel dextransucrase is produced by *Leuconostoc citreum* strain B/110-1-2: An isolate used for the industrial production of dextran and dextran-derivatives. *J. Ind. Microbiol. Biotechnol.* **2011**, *38*, 1499–1503. [\[CrossRef\]](#)
21. Fraga, R.; Pacios, S.; Arísticas, R.C.; Martínez, L.; Lafargue, M.; Montes, A.; Remaud-Simeon, M.; Monsan, P. Cloning and Partial Characterization of an Extracellular Dextransucrase Coding Region (DSR-V) from *Leuconostoc citreum* M-3. In *Microbial Exopolysaccharides: Current Research and Developments*, 1st ed.; Duru, Ö.A., Ed.; Caister Academic Press: Norfolk, UK, 2019; Chapter 11; pp. 295–314. [\[CrossRef\]](#)
22. Joucla, G.; Pizzut, S.; Monsan, P.; Remaud-Simeon, M. Construction of a fully active truncated alternansucrase partially deleted of its carboxy-terminal domain. *FEBS Lett.* **2006**, *580*, 763–768. [\[CrossRef\]](#)
23. Olivares-Illana, V.; López-Munguía, A.; Olvera, C. Molecular characterization of inulosucrase from *Leuconostoc citreum*: A fructosyltransferase within a glucosyltransferase. *J. Bacteriol.* **2003**, *185*, 3606–3612. [\[CrossRef\]](#) [\[PubMed\]](#)
24. Vuillemin, M.; Claverie, M.; Brison, Y.; Séverac, E.; Bondy, P.; Morel, S.; Monsan, P.; Moulis, C.; Remaud-Siméon, M. Characterization of the first α -(1 \rightarrow 3) branching sucraes of the GH70 family. *J. Biol. Chem.* **2016**, *291*, 7687–7702. [\[CrossRef\]](#) [\[PubMed\]](#)
25. Parlak, M.; Ustek, D.; Tanriseven, A. Designing of a novel dextransucrase efficient in acceptor reactions. *Carbohydr. Res.* **2014**, *386*, 41–47. [\[CrossRef\]](#) [\[PubMed\]](#)
26. Hong, J.; Wang, Y.; Ye, X.; Percival Zhang, Y.H. Simple protein purification through affinity adsorption on regenerated amorphous cellulose followed by intein self-cleavage. *J. Chromatogr. A* **2008**, *1194*, 150–154. [\[CrossRef\]](#)
27. Meng, X.; Dobruchowska, J.M.; Pijning, T.; Gerwig, G.J.; Kamerling, J.P.; Dijkhuizen, L. Truncation of domain V of the multidomain glucansucrase GTF180 of *Lactobacillus reuteri* 180 heavily impairs its polysaccharide-synthesizing ability. *Appl. Microbiol. Biotechnol.* **2015**, *99*, 5885–5894. [\[CrossRef\]](#)
28. Molina, M.; Moulis, C.; Monties, N.; Pizzut-Serin, S.; Guieysse, D.; Morel, S.; Cioci, G.; Remaud-Simeon, M. Deciphering an undecided enzyme: Investigations of the structural determinants involved in the linkage specificity of alternansucrase. *ACS Catal.* **2019**, *9*, 2222–2237. [\[CrossRef\]](#)
29. Moulis, C.; Joucla, G.; Harrison, D.; Fabre, E.; Potocki-Veronese, G.; Monsan, P.; Remaud-Simeon, M. Understanding the polymerization mechanism of glycoside-hydrolase family 70 glucansucraes. *J. Biol. Chem.* **2006**, *281*, 31254–31267. [\[CrossRef\]](#)
30. Molina, M.; Moulis, C.; Monties, N.; David, G.; Morel, S.; Cioci, G.; Remaud-Simeon, M. A specific oligosaccharide-binding site in the alternansucrase catalytic domain mediates alternan elongation. *J. Biol. Chem.* **2020**, *295*, 9474–9489. [\[CrossRef\]](#) [\[PubMed\]](#)
31. Tsuchiya, H.M.; Hellman, N.N.; Koepsell, H.J. Factors affecting the molecular weight of enzymatically synthesized dextran. *J. Am. Chem. Soc.* **1953**, *75*, 757–758. [\[CrossRef\]](#)
32. Bechtner, J.; Hassler, V.; Wefers, D.; Vogel, R.F.; Jakob, F. Insights into extracellular dextran formation by *Liquorilactobacillus nagelii* TMW 1.1827 using secretomes obtained in the presence or absence of sucrose. *Enzyme Microb. Technol.* **2021**, *143*, 109724. [\[CrossRef\]](#) [\[PubMed\]](#)
33. Zhang, Y.-H.P.; Cui, J.; Lynd, L.R.; Kuang, L.R. A transition from cellulose swelling to cellulose dissolution by *o*-phosphoric acid: Evidence from enzymatic hydrolysis and supramolecular structure. *Biomacromolecules* **2006**, *7*, 644–648. [\[CrossRef\]](#)
34. Sumner, J.; Howell, S. A method for determination of invertase activity. *J. Biol. Chem.* **1935**, *108*, 51–54. [\[CrossRef\]](#)
35. Bradford, M.M. A rapid and sensitive method for the quantitation of microgram quantities of protein utilizing the principle of protein-dye binding. *Anal. Biochem.* **1976**, *72*, 248–254. [\[CrossRef\]](#)
36. Miller, A.W.; Robyt, J.F. Detection of dextransucrase and levansucrase on polyacrylamide gels by the periodic acid-Schiff stain: Staining artifacts and their prevention. *Anal. Biochem.* **1986**, *156*, 357–363. [\[CrossRef\]](#)
37. Fernandez-Patrón, C.; Hardy, E.; Seoane, J.; Castellanos, L. Double staining of Coomassie blue-stained polyacrylamide gels by imidazole-sodium dodecyl sulfate-zinc reverse staining: Sensitive detection of Coomassie blue-undetected proteins. *Anal. Biochem.* **1995**, *224*, 263–269. [\[CrossRef\]](#)